

# Fluorescent Carbon Dots for Selective Labeling of Subcellular Organelles

Binesh Unnikrishnan, Ren-Siang Wu, Shih-Chun Wei, Chih-Ching Huang,\* and Huan-Tsung Chang\*



Cite This: *ACS Omega* 2020, 5, 11248–11261



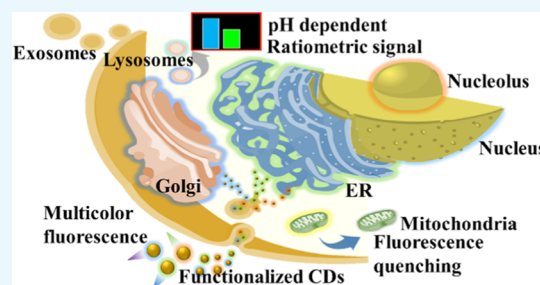
Read Online

ACCESS |

Metrics & More

Article Recommendations

**ABSTRACT:** With the recent advancement in understanding and control of the structure and optical properties of fluorescent carbon dots (CDs), they have been shown to be valuable in biolabeling of bacteria, tumor cells, tissues, and organelles. Their extremely small size and tunable functional properties coupled with ultrastable fluorescence enable CDs to be used for easy and effective labeling of various organelles. In addition, CDs with advantages of easy preparation and functionalization with recognition elements and/or drugs have emerged as nanocarriers for organelle-targeted drug delivery. In this review, we mainly discuss the applications of fluorescent CDs for the labeling of organelles, including lysosome, nucleoli, nucleus, endoplasmic reticulum, and mitochondria. We highlight the importance of the surface properties (functional groups, hydrophobicity/hydrophilicity, charges, zwitterions) and the size of CDs for labeling. Several interesting examples are provided to highlight the potential and disadvantages of CDs for labeling organelles. Strategies for the preparation of CDs for specific labeling of organelles are suggested. With the edge in preparation of diverse CDs, their potential in labeling and drug delivery is highly expected.



## 1. INTRODUCTION

Selective staining of the subcellular structure of organelles can provide vital information about the status, functionality, and metabolism of cells, as well as their responses to therapy and external stimuli.<sup>1</sup> Although organic dyes are most commonly used for staining of subcellular organelles, they still have many drawbacks such as limited excitation/emission wavelengths, poor photostability, and low biocompatibility.<sup>2,3</sup> Their low photostability restricts the long-term monitoring of dynamic changes of cellular functions and structures. Most fluorescent dyes, comprising organic fluorophores, are susceptible to photobleaching due to irreversible photodamage in their structures. Although several antifade mountants and reductants for fixed and living cells have been developed to minimize the fluorescent dyes from photobleaching, further steps required are troublesome.<sup>2,4</sup> Immuno-based labeling technologies achieve precise organellar labeling, but the high cost of assay kits, laborious analysis steps, and experienced personnel are often necessary.<sup>5</sup> Thus, fluorescent labeling materials with improved resistance against photobleaching would hold great potential in future fluorescence imaging applications.

Since carbon dots (CDs) prepared from glycine through a hydrothermal route were used for cell labeling (Figure 1),<sup>6</sup> numerous types of fluorescent CDs synthesized from different precursors and different methods have been developed as cell imaging reagents.<sup>7–9</sup> CDs can be used for imaging of both living and apoptotic cells.<sup>10–12</sup> They can be prepared from a variety of carbon sources from pure compounds such as glycine

and citric acid to cheap and organic waste such as used coffee ground, leaves, and cow manure.<sup>6,8,10,13–15</sup> Detailed reviews of the bioimaging and diagnostic application of CDs are available.<sup>11,12,16–18</sup> Having the advantages of brilliant photostability and excitation-dependent emission, CDs can realize long durations of imaging and full-color fluorescence imaging of cells.<sup>19,20</sup> The high photostability and biocompatibility of CDs enable living cell imaging of bacterial and mammalian cells.<sup>21,22</sup> For mammalian cells, most of the CDs can achieve cytoplasmic accumulation rather than specific organelle distribution. The dynamic properties of cellular membranes have a strong effect on the interaction and endocytosis of the CDs.<sup>23</sup> CDs exhibit high biocompatibility, which makes them more suitable than other staining agents such as organic dyes, fluorescent proteins, and (semiconductive) metal-based quantum dots for biolabeling applications. In addition, their excellent photostability allows long-term monitoring of dynamic cellular processes.<sup>24</sup> Excitation wavelength-dependent emission properties of fluorescent CDs provide advantages of multicolor imaging of cells or organelles.<sup>25,26</sup> Furthermore, the

Received: December 17, 2019

Accepted: April 24, 2020

Published: May 5, 2020



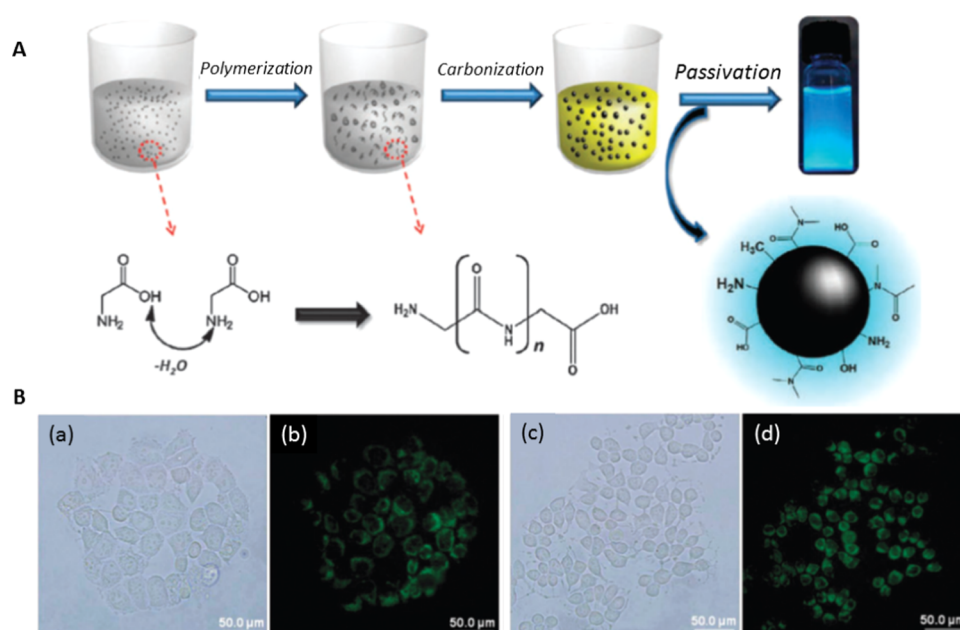
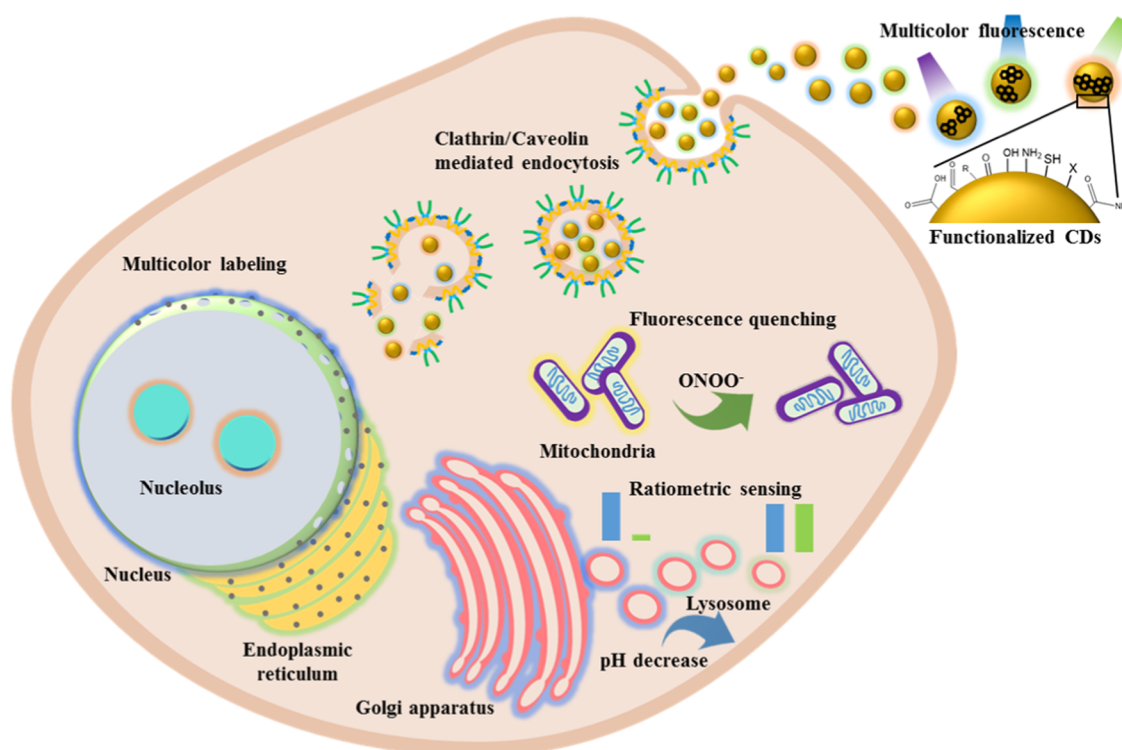


**Figure 1.** (A) Schematic representation for the synthesis of CDs from glycine. (B) Bright-field and fluorescence images of MCF-10A (a, b) and MCF-1 (c, d) cells treated with hydrophilic fluorescent CDs. Reproduced with permission from ref 6. Copyright 2012 Royal Society of Chemistry.

### Scheme 1. Schematic Representation of Endocytosis of Fluorescent CDs and Specific Labeling of Various Organelles and Their Imaging by Different Fluorescence Techniques



pH-dependent emission properties of CDs enable the detection of intracellular pH with appreciable accuracy.<sup>27</sup> Some studies suggest that hydrophilicity, functional groups, and surface charges of the CDs are important for their internalization into the cells and targeting of organelles.<sup>26–29</sup> The surface properties of CDs can be controlled during the synthesis process and postmodification, which are necessary for specific organelle labeling or drug delivery after endocytosis. A schematic representation of the endocytosis followed by

labeling of different organelles with CDs, and monitoring through various fluorescence techniques, including multicolor imaging, ratiometric imaging, fluorescence quenching, and pH-dependent emission, is presented in Scheme 1. However, a clear understanding of the properties of CDs for specific interactions with organelles is not yet available. In this review, we discuss various types of CDs employed for labeling of different subcellular organelles and the properties of CDs that are essential for targeting.

## 2. LABELING OF ORGANELLES WITH FLUORESCENT CDS

CDs have been successfully applied for the labeling of bacterial cells and cancer cells as well as for tissue imaging.<sup>16,30–32</sup> Most reported CDs remain in the cytoplasm after internalization. Internalization of the fluorescent CDs is mainly due to the endocytosis mechanism; meanwhile, the specificity is achieved either with the help of target-specific functionalization or by intrinsic functional groups on the CDs preserved from their precursors. Since various organelles possess different membrane properties and internal biochemistry, CDs with specific characteristics, such as size, functional groups, biocompatibility, and suitable surface charge, are required for targeting the organelle membrane or internalization. For example, CDs with amino groups (with a weak positive charge) are found to target lysosomes;<sup>27</sup> however, a slight modification of amine-functionalized CDs with lipophilic molecules such as laurylamine can change the target to the endoplasmic reticulum (ER), due to differences in the endocytosis mechanism.<sup>33</sup> However, highly positively charged or heterogeneously charged CDs (having both positive and negative charges) target the nucleus and nucleolus.<sup>34,35</sup> However, there are some contradictory findings regarding the surface charge and nucleus-targeting ability of the CDs.<sup>36,37</sup> Therefore, for convenience, we categorized the following sections based on organelles. We mainly focus our discussion on correlating the physicochemical properties of CDs and their specificity in targeting subcellular structures. The major organelles and subcellular structures studied for CD-based labeling applications are lysosomes, nucleus, nucleolus, mitochondrion, ER, exosomes, and Golgi apparatus.

**2.1. Lysosomes.** Lysosomes are spherical, membrane-enclosed organelles found in animal cells, with environmental pH values of 4.5–5.5. They contain many enzymes, such as phosphatases, nucleases, polysaccharide hydrolase, proteases, and lipid-degrading enzymes, and are involved in various cellular processes, such as autophagy, endocytosis, hydrolysis of large molecules, and so on. Abnormal pH changes in the lysosome can provide information regarding the cellular healthy conditions. pH and morphology changes of lysosomes during cell apoptosis and oncogenic transformation have been found.<sup>38,39</sup> Therefore, a probe with a sensitive pH-dependent emission response is a prerequisite for lysosome labeling that can provide vital information for understanding the dysfunction of lysosomes, which might relate to various pathologies, including neurodegenerative diseases, cancer, and Alzheimer's diseases. CDs have been used as a drug carrier for targeting the lysosome of cancer cells as well as for photothermal therapy (PTT).<sup>40</sup> CDs cofunctionalized with the lysosome-targeting ruthenium nitrosyl donor (Lyso-Ru-NO) for specifically targeting lysosomes and delivering nitric oxide and with the cancer cell-targeting ligand (folic acid) were prepared for cancer cell therapy.<sup>40</sup> The Lyso-Ru-NO contains a ligand of Lyso-NINO (a lysosome-specific two-photon fluorescent probe known to detect endogenous NO in cells), in which the morpholine (ML) moiety serves as a lysosomal targeting group. The small size of the CDs (7–9 nm) makes them suitable carriers for targeting subcellular organelles, and their photoluminescence enables visualization of the intracellular tracking of the drug delivery system. Under the laser irradiation at 808 nm, it induces NO release and a rapid increase in temperature, resulting in a synergistic therapy for cervical cancer cells (HeLa cells). More recently, Wu et al. reported

that polyethyleneimine (PEI)-passivated CDs functionalized with ML is an effective probe for multicolor labeling of lysosomes in live HeLa cells.<sup>26</sup> The surface-bound PEI enhances the fluorescence quantum yield (QY) and photostability; meanwhile, the ML engages in targeting lysosomes. In addition, the study reveals that the internalization of the functional CDs is through the endocytic pathway and accumulation in the lysosome, making it an efficient probe for labeling lysosomes.

CDs rich in amino groups can specifically target lysosomes, without any tedious lysosome-targeting postmodification.<sup>27</sup> In addition, CDs can also be used for monitoring the pH of lysosomes based on their pH-sensitive fluorescence properties. For example, amine-rich CDs synthesized from *p*-benzoquinone and ethanediamine were employed for targeting lysosomes and for real-time monitoring of pH in lysosomes.<sup>27</sup> The fluorescence intensity of CDs dramatically decreases in a medium upon decreasing pH values from 6.0 to 4.0, which is appropriate for investigating the pH changes of lysosomes. The pH-dependent fluorescence intensity of the CDs is mainly due to reversible protonation and deprotonation of their functional groups including amino groups and other hydrophilic groups such as carboxylate groups evident from  $\zeta$  potential measurements. The CDs were further applied to monitor lysosomal pH changes during dexamethasone-induced apoptosis of A549 cells (adenocarcinomic human alveolar basal epithelial cells). Not only CDs with amino groups, graphene quantum dots (GQDs) prepared from extracts of neem plant root by a solvothermal method, with surface functional groups, such as  $-\text{NH}_2$ ,  $-\text{COOH}$ , and  $\text{C}-\text{O}-\text{C}$ , also have been reported to possess good lipophilicity and to be specific for targeting lysosomes.<sup>41</sup> Further, the GQDs are suitable for two-photon excitation microscopy, enabling long-time imaging with less damage to living RAW cells. The presence of  $-\text{NH}_2$ ,  $-\text{COOH}$ , and  $\text{C}-\text{O}-\text{C}$  groups is suggested to be the main reason for both lipophilicity and specific targeting of the lysosome; however, more experimental evidence is required to prove the exact interactions leading to specific targeting.

Ratiometric imaging is based on the use of a ratio between two fluorescence intensities. The nanoprobe-based ratiometric imaging is often more refined and reliable than the traditional one due to the fact that bleaching, changes in focus, variations in laser intensity as well as the physiological conditions of cells can be corrected. Owing to their easy functionalization and surface manipulation, fluorescent CDs can be used to immobilize an additional fluorescent probe to construct a ratiometric signal recording strategy for labeling of organelles.<sup>42,43</sup> For example, naphthalimide derivative-functionalized CDs have been used for imaging and monitoring of endogenous formaldehyde in lysosomes in live cells (Figure 2A).<sup>42</sup> The ratio of green fluorescence (535 nm) from the naphthalimide derivative to blue fluorescence (414 nm) from CDs is correlated to the concentration of formaldehyde in lysosomes. Lysosomes play significant roles in endogenous formaldehyde generation, in which high levels of formaldehyde play diverse roles in many diseases such as Alzheimer's disease, reproductive and developmental toxicities, and cancer.<sup>44–46</sup> The imaging of HeLa cells is in response to the increased formaldehyde concentration, with an enhanced green fluorescence intensity of naphthalimide derivative and a constant fluorescence intensity of the CDs as shown in Figure 2B.<sup>42</sup> The naphthalimide derivative undergoes a simple diffusion process to enter the cell and can also target other



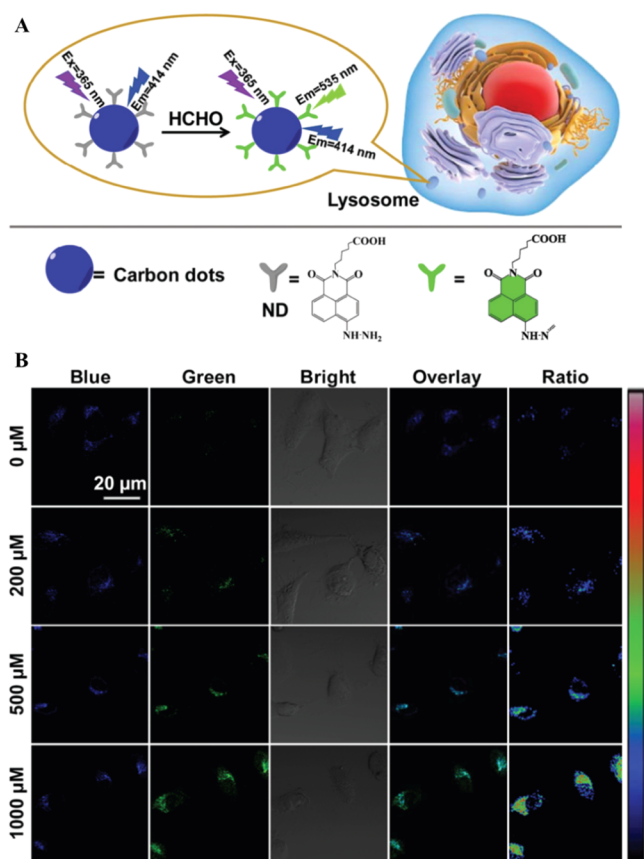


**Figure 2.** (A) Schematic representation for the design of CDs functionalized with naphthalimide for targeting lysosome and ratiometric imaging. (B) Confocal laser microscopic images of HeLa cells treated with different concentrations of formaldehyde and labeled with naphthalimide-modified CDs. Reproduced with permission from ref 42. Copyright 2019 Royal Society of Chemistry.

organelles without specificity. Endocytosis of the naphthalimide derivative-functionalized CDs is believed to happen through clathrin- and caveolae-mediated pathways, which are active transportation mechanisms, and the presence of weakly basic amino groups on the CDs enhances the lysosome-targeting efficiency. The acidic environment inside the lysosome induces aggregation of the amine-rich CDs, which enhances their accumulation.

CDs alone can also be employed for ratiometric signal acquisition, without an additional fluorescent molecule, by utilizing the analyte-dependent emission wavelength shift of the CDs. CDs synthesized from dexamethasone and 1,2,4,5-benzenetetramine as precursors through a microwave-assisted hydrothermal method exhibit red fluorescence through the intramolecular charge transfer (ICT) mechanism.<sup>43</sup> Upon their interaction with formaldehyde, the CDs exhibit green fluorescence through decreases in ICT. The residual *o*-diamino groups on the CDs react selectively with formaldehyde, leading to ratiometric fluorescence response through decreases in the ICT process from the electron-donating amino group to the electron-withdrawing carbonyl group of CDs. The formaldehyde-induced blue shift in the fluorescence wavelength is ideal for developing a ratiometric sensing system for the detection of formaldehyde in the lysosome, showing their potential for specific targeting of lysosomes.

Reliability of the ratiometric lysosome labeling and determination of pH values in lysosomes can be further improved by functionalizing the fluorescent CDs with a pH-dependent fluorescent molecule with the same/close excitation wavelength as that of fluorescent CD.<sup>47</sup> He et al. demonstrated that upon excitation with a wavelength of 380 nm at the pH from 4.0 to 8.0, the emission of CDs at 455 nm remains almost constant, whereas the 1,8-naphthalimide derivative fluorophore on the CDs gradually decreases at 525 nm.<sup>47</sup> The ratio of these two fluorescence responses of 1,8-naphthalimide derivative-functionalized CDs with respect to pH change allows for constructing an efficient ratiometric sensor for monitoring pH values in lysosomes.

Hydrophilicity of CDs has been reported to be a vital factor for the labeling of organelles.<sup>27</sup> In contrast, Mao et al. demonstrated the labeling of lysosomes with hydrophobic CDs (~8.5 nm) containing short alkyl groups prepared from an ionic liquid 1-ethyl-3-methylimidazolium bromide by a hydrothermal method.<sup>48</sup> Interestingly, the hydrophobic CDs can penetrate into HeLa cells within 1 min and are mainly distributed in the lysosome. In contrast to hydrophilic CDs, the penetration behavior of the hydrophobic CDs shows partially energy-dependent and passive diffusion. The Fourier transform infrared (FT-IR) and X-ray photoelectron spectroscopy (XPS) spectra reveal C–N, C=N, C–O, C=O, and C–O–C groups are present in the CDs. Thus, the notion that the lysosome-targeting ability mainly arose from the hydrophobicity of the CDs should be further investigated.

In addition to CDs and N-doped CDs, metal-incorporated CDs are also found to be effective in targeting the lysosome. Near-infrared (NIR) emissive CDs prepared by carbonization of Mn(III)tetra-(*meso*-aminophenyl)porphyrin with citric acid (MnPCNDs) have specific lysosome-targeting properties.<sup>49</sup> In addition to targeting and then accumulation in the lysosome, these MnPCNDs when irradiated with an NIR laser exhibit an excellent photodynamic therapeutic (PDT) effect for tumor cell therapy. Moreover, the MnPCNDs containing paramagnetic Mn(III) ions make them a  $T_1$ -weighted magnetic resonance imaging (MRI) contrast agent for *in vivo* tumor monitoring and PDT guidance. In addition, metal complex-modified CDs such as Ru(II)complex-functionalized CDs (Ru1-CDs) have been reported to penetrate into cancer cells through the endocytosis mechanism, with features of targeting of lysosomes as well as possessing a promising PDT effect through one- or two-photon excitation.<sup>50</sup> The CDs act as an efficient carrier that greatly enhances the cellular uptake efficacy of the photosensitizer Ru1. Although the uptake of both Ru1 and Ru1-CDs is reported to be through an energy-dependent mechanism, the exact mechanism behind the increased uptake efficacy of Ru1-CDs has not been discussed clearly.

In summary, surface functionalization of CDs with ligands containing a morpholine moiety can be used for specific lysosome targeting. In addition, amine-rich CDs, and both hydrophilic and hydrophobic CDs, are found to be viable for lysosome labeling. Thus, the specificity of those CDs for lysosome labeling is still controversial. Although some reports showed the Pearson correlation coefficients to prove the good overlaps between the CDs and LysoTracker probes, the locations of the CDs and LysoTracker probes should be different. LysoTracker probes for lysosome labeling are likely to be involved in the protonation and retention in the membranes of organelles. The cellular uptake of CDs is



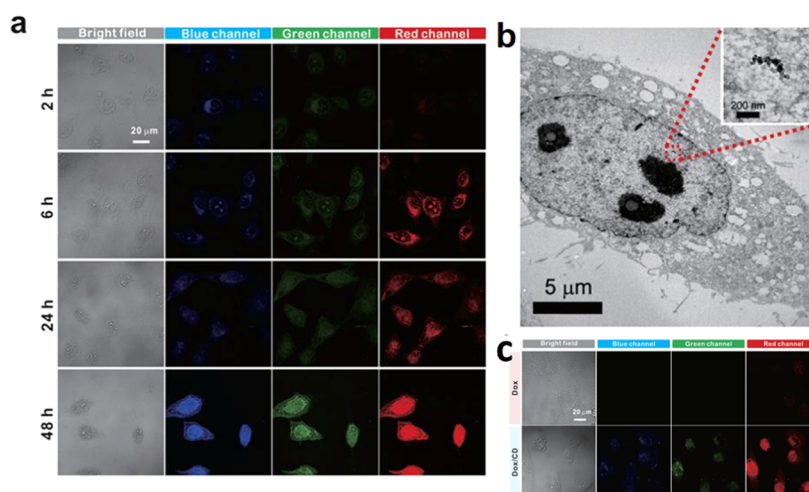


**Figure 3.** Nucleus staining of HeLa cells with zwitterionic CDs. (a) Bright-field and confocal fluorescence microscopy images for different incubation times to show the cytoplasmic and nuclear transport of CDs. (b) Biotransmission electron microscopic image showing localization of CDs in the nucleus. (c) Bright-field and confocal fluorescence images of HeLa cells treated with DOX and DOX/CD. Reproduced with permission from ref 29. Copyright 2015 Springer Nature.

believed to be through energy-dependent and *via* micropinocytosis, caveolae- and clathrin-mediated pathways prior to transportation to lysosomes. Therefore, most CDs with various functional groups can be transiently localized in lysosomes. Although the CDs with high surface abundance of amino groups exhibit superior lysosome-labeling efficacy, they can target the ER as well. Thus, the specificity of CDs for targeting the lysosome and long-term real-time monitoring of the alternation of pH in the lysosome using CDs still remains a challenge.

**2.2. Nucleus.** Targeting the nucleus for drug delivery is essential, especially for cancer therapy, in which the drug interferes with the proliferation of cancer cells. CDs have been found to be an efficient agent for nucleus labeling and a nanocarrier for nucleus-targeted therapy without or with postmodification of nuclear-targeting ligands.<sup>28,29,34,36,51–60</sup> For example, N-doped CDs synthesized from ascorbic acid and branched polyethyleneimine with small sizes (~4 nm) and a zwitterionic surface are efficient for internalization and targeting of the nucleus.<sup>53</sup> Zwitterionic nanoparticles with high colloidal stability over a wide pH range and resistant to nonspecific adsorption of proteins have prolonged blood circulation to enhance their accumulation in tumors. Zwitterionic CDs synthesized from citric acid as a carbon source and  $\beta$ -alanine as a zwitterionic passivating agent also allow cytoplasmic uptake and subsequent delivery to the nucleus.<sup>29</sup> The excitation-dependent emission of the CDs enables multicolor imaging of the nucleus in HeLa cells, which shows the internalization of the CDs with different times of incubation (Figure 3). These CDs were also used to accelerate drug delivery of doxorubicin (DOX). Nucleus-targeting drug delivery plays a crucial role in the treatment of tumors as these drugs cause gene damage and disrupt the proliferation of the cancer cells. CDs prepared by the hydrothermal processing of milk have been successfully applied for the pH-dependent release of DOX into the nucleus.<sup>54</sup> DOX is physically adsorbed on the CDs through electrostatic interaction and is released in the nucleus after localization. The free CDs and free DOX are mainly distributed in the cytoplasm of the cell, with some amounts of CDs in the nucleus and DOX in the nuclear membrane. A detailed study regarding the mechanism of

nucleus targeting and internalization of CDs is however lacking. Another study demonstrated that the CDs synthesized from glycerol passivated with polyamine-containing organosilane and modified with DOX *via* amide bonds could efficiently deliver the DOX into the nucleus, while the CDs remain in the cytoplasm.<sup>60</sup> Hydrolysis of amide bonds by hydrolases such as carboxylesterases and acid-catalyzed hydrolysis in intracellular lysosomes/endosomes is the main reason for inducing the release of DOX from CDs. Recently, Hill et al. reported that CDs noncovalently capped with 2,5-deoxyfructosazine prepared through microwave heating of glucosamine and *m*-phenylenediamine exhibit high nucleus-targeting efficiency. Irradiation of the CD-internalized cancer cells using a blue light-emitting diode (LED) (460 nm) enhances the killing activity of the CDs by increasing the intracellular localized temperature followed by adenosine 5'-triphosphate (ATP) depletion.<sup>51</sup> However, specificity for targeting of the nucleus is inefficient; the average global Pearson coefficient of the CDs for the nucleus was only 0.62.

Self-assembled CDs (~70–90 nm at neutral pH, and the size decreases to ~48 nm at pH 3) prepared from a grape seed extract by microwave heating without any functionalization were found to internalize into the cells through caveolae- and clathrin-mediated endocytosis and then target the nucleus.<sup>36</sup> Disassembly of the self-assembled CDs to form extremely small sizes of CDs having negative charges is responsible for nucleus-specific localization. In contrast, graphene CDs passivated with branched PEI, with a small size (1.66 nm) and high positive charge, also have been reported to exhibit high nucleus permeability.<sup>34</sup> CDs prepared from dopamine have been reported to have high nitrogen doping and surface amino groups with a  $\zeta$  potential of +12.8 mV, which have high penetration efficiencies into the nucleus of various cancer cell lines.<sup>28</sup> In addition to positively charged CDs, Liu et al. showed that neutral CDs are distributed in the entire cell including the nucleus, whereas negatively charged CDs are located in the cytoplasm only, indicating that the net charge of CDs has a significant role in targeting the organelle.<sup>56</sup>

Another advantage of CDs is their intrinsic ability to distinguish cancer cells from normal cells through specific organelle labeling. CDs synthesized from *o*-phenylenediamine

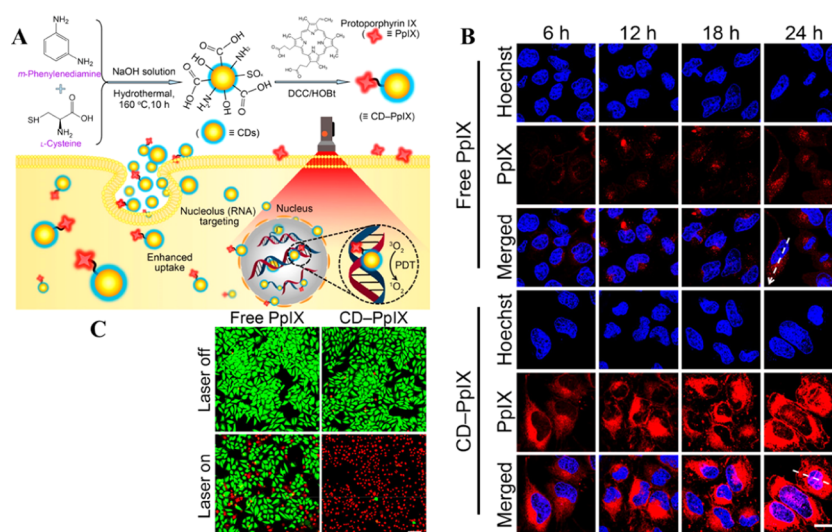


**Figure 4.** (A) Schematic of the synthesis of CDs and their nucleolus imaging and drug delivery mechanism. (B) Confocal microscopic images showing the drug delivery efficiency of the CDs for HeLa cells. (C) Live/dead staining results of HeLa cells treated with free PpIX and PpIX-CDs before and after laser irradiation. Reproduced with permission from ref 37. Copyright 2018 American Chemical Society.

are reported to internalize into the cytoplasm and nucleus of hepatoma cells (HepG2) within 3 min.<sup>59</sup> The fast internalization and high uptake are believed to be due to small sizes (~4 nm) of the CDs and abundant carboxylate and amino groups on their surfaces. The CDs exhibit a  $\zeta$  potential of *ca.* -10 mV at pH 7.4, which reduces nearly to zero at pH 5.0. Therefore, the protonation of the endocytic CDs causes an influx of water into the endosomes and their disintegration, which paves the way for the fast escape of CDs from endosomes and then their localization in the nucleus. The study further showed that the CDs distinguish hepatoma cells (HepG2) from normal human liver cells (LO2) through specific staining of the nucleus of the HepG2 cells only. This phenomenon is probably due to differences in cellular pH values, as well as in the endosomal-lysosomal system and nucleoporins of nuclear pore complexes between normal and cancer cells. Certain types of cancer cells (*e.g.*, HeLa, HepG2, MCF-7) overexpress folate receptors on their membrane, and therefore, functionalizing CDs with folic acid is a popular strategy to target and identify folate receptor-overexpressed cancer cells.<sup>30,58</sup>

Reports on the surface properties of CDs for the specific labeling of the nucleus are inconsistent. Some studies propose that the zwitterionic surfaces of CDs are responsible for the nucleus targeting, while small-sized graphene CDs with negative charges or CDs with positive charges also have been found to localize in the nucleus. Moreover, though these reports demonstrate the use of CDs for targeting the nucleus, functional characteristics of CDs essential for specific targeting of the nucleus or nucleus membrane have not been understood completely yet. The contradictory reports of surface charge for nucleus-specific targeting of CDs could be due to the difference in the protonation/deprotonation of the functional groups and changes in the  $\zeta$  potential of the endocytic CDs, which have to be studied more carefully to obtain detailed information about the targeting of CDs toward the nucleus.

**2.3. Nucleolus.** Nucleoli are subcellular organelles in nuclei, which play a crucial role in the synthesis of ribosomal RNA (rRNA) and assembly of ribosomal subunits with rRNA.<sup>61</sup> Ribosomes are responsible for the production of

polypeptides and proteins. In general, transformed cells, cancerous cells, and immune activated cells produce kinases and transcription factors for proliferation and propagation.<sup>56</sup> In these cells, increased quantities and larger sizes of nucleoli are usually found as a result of more production of rRNA in nucleoli by RNA polymerase I. Therefore, the quantities and sizes of nucleoli can be used as indicators for monitoring the cellular status.<sup>62</sup> Traditional methods, such as immunohistochemistry (IHC),<sup>63</sup> fluorescence *in situ* hybridization (FISH),<sup>64</sup> silver staining,<sup>65</sup> and organic fluorophores,<sup>66</sup> are often used to study nucleolar morphologies. However, IHC, FISH, and silver staining are limited to the staining of nucleoli in fixed cells, whereas many organic fluorophores, such as RNA dye (SYTO RNASelect green fluorescent cell stain), are available to label both living and fixed cells.<sup>67</sup> Despite the versatility of RNA dyes in the staining of living and fixed cells, the susceptibility of organic dyes to photobleaching is problematic, which limits the applications of organic dyes in long durations of cell imaging. Although most fluorescent CDs can achieve cellular labeling and cytoplasmic accumulation, their nucleolar distribution is still difficult. Fluorescent CDs with charge heterogeneity on their surfaces have been explained for their penetrating the nucleus and preferential binding with nucleoli in HeLa and LN229 cells.<sup>35</sup> CDs with both positive and negative charges on their surface (*i.e.*, charge heterogeneity) can enter the cytoplasm and nucleus and are preferentially distributed in the nucleoli due to favorable interaction with RNA. Since the nucleolus is abundant in RNA, nucleolar-specific labeling is also possible with CDs having a high affinity toward RNA. For example, CDs synthesized from citric acid and urea allow nuclear-specific labeling through their RNA-binding property and accumulation in nucleoli, which was supported by conducting an RNA digestion test.<sup>68</sup> An exact interaction mechanism between CDs and RNA is unavailable though it is speculated that RNA forms a chemical bonding with CDs through the 2'-hydroxyl group on its pentose ring. Hua et al. demonstrated nucleolus targeting using negatively charged CDs synthesized from *m*-phenylenediamine and L-cysteine, which also act as a platform for drug delivery.<sup>37</sup> Schematic representation of the synthesis methods of CDs and

the internalization into the nucleolus is given in Figure 4A. The electrostatic interaction between CDs and RNA as a reason for nucleolar targeting can be ruled out because they both have negative charges. In addition, this study further demonstrated that the CDs conjugated with a photosensitizer (protoporphyrin IX) effectively increased the cellular uptake and nucleus-targeting and provided an enhanced phototherapeutic effect because of poor tolerance of the nuclei to reactive oxygen species (ROS) produced during the PDT (Figure 4B).

Recently, CDs prepared from *p*-phenylenediamine (*p*PDA) with metal ions, such as Ni<sup>2+</sup> ions as the catalyst (Ni-pPCDs) with red fluorescence emission at 600 nm, have been reported to specifically illuminate the nucleoli in A549 cells.<sup>69</sup> The specificity is reported to be due to the electrostatic interaction between the positively charged Ni-pPCDs ( $\zeta$  value of  $\sim 24$  mV) and negatively charged RNA in the nucleolus. The Ni-pPCDs could be used for imaging of both living and fixed cells, and their photostability is much better than the commercial dye, SYTO RNASelect. In addition, the authors showed that Ni-pPCDs can pass through the mucus layer of the zebrafish embryo and achieve whole zebrafish imaging due to the positive charge and amphiphilicity of the CDs. Fluorescent CDs can also be used for simultaneous tracking of DNA and RNA, mainly due to the affinity of the CDs, the rigidity of DNA, and flexibility of RNA.<sup>70</sup> Han et al. developed a CD-based probe by functionalizing the CDs with *p*-phenylenediamine (*p*PDA) and 4-carboxybutyl triphenylphosphonium (PPh<sub>3</sub><sup>+</sup>) bromide. The CDs show different responses toward double-stranded DNA (dsDNA) and single-stranded RNA (ssRNA), which enable real-time monitoring of DNA and RNA.<sup>70</sup> The functionalization increases the surface positive charge of the CDs to a  $\zeta$  potential value of +20 mV, which allows their strong interaction with the nucleic acids. The report suggested that blue fluorescence of the disclike nanostructured graphene CDs (diameter  $\sim 3$  nm; thickness  $\sim 1$  nm) at 510 nm increases upon insertion into the grooves of dsDNA, which is similar to some DNA intercalating dyes. However, the insertion of the graphene CDs into the grooves of dsDNA is implausible since the thickness of CDs ( $\sim 1$  nm) is much larger than that of the major groove (0.22 nm) and minor groove (0.12 nm) of dsDNA. On the other hand, the CDs interact with the flexible ssRNA, resulting in their accumulation in close proximity and thus leading to red-shifted fluorescence. The CDs have planar disclike structures, which enable  $\pi$ - $\pi$  stacking when the CDs are in close proximity and further result in boosting red-shifted fluorescence. The CDs were employed for staining of the nucleus with green emission and the nucleolus with red emission (Figure 5).<sup>70</sup> With the graphene CDs' imaging results validated in live cells, the CDs were further applied to study the DNA and RNA structures during cell division. In addition, the photostable graphene QDs allow time-lapse imaging of chromatin and nucleoli during cell division and *Caenorhabditis elegans* growth when applying super-resolution microscopy. Although the CDs work nicely for labeling of DNA and RNA, the proposed interactions (electrostatic interaction,  $\pi$ - $\pi$  stacking, and hydrogen bonding) of graphene CDs with dsDNA and ssRNA require more detailed study,

Temperature-dependent fluorescence properties of CDs have been utilized as nanothermometers in living cells and in nucleolar staining.<sup>71</sup> The fluorescence intensity of CDs synthesized from ascorbic acid by an electrochemical method exhibits linear decreased response from 20 to 100 °C. Further,

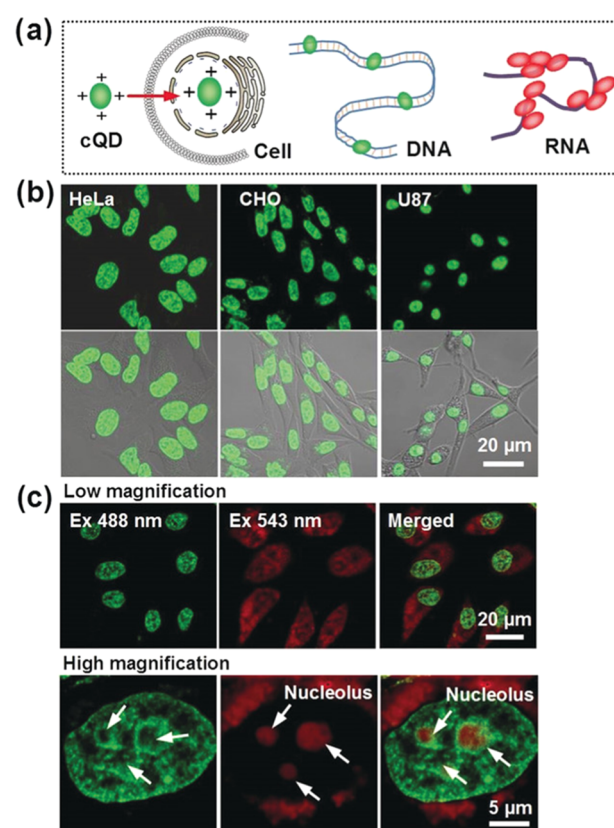


**Figure 5.** (a) Schematic of CDs binding to DNA and RNA. (b) Fluorescence images of different cell lines treated with CDs for nucleus imaging. (c) Multicolor fluorescence imaging of HeLa cells with the CDs using multiple excitation and emission wavelengths. Reproduced with permission from ref 70. Copyright 2019 Wiley-VCH.

the CDs have nucleolar staining ability through their interaction with DNA and RNA molecules, leading to their enrichment in the nucleolar region. Similarly, red emissive carbon quantum dots ( $\lambda_{\text{max}} \approx 640$  nm) synthesized from citric acid in formamide exhibit nucleolar staining, due to their strong interaction with RNA in the nucleolus.<sup>72</sup> The CDs were further used for delivery of fluorescein isothiocyanate and for photothermal therapy. Although the localization of the CDs in the nucleolus is supported by ribonuclease digestion testing, the exact mechanisms behind the noncovalent interaction of CDs and RNA are unavailable.

In summary, the nucleolus-targeting abilities of the CDs are mainly attributed to their interaction with the RNA in the nucleoli, which leads to the accumulation of the CDs in the nucleolar region. The affinity of these CDs toward RNA molecules is deduced to arise from various noncovalent interactions, including hydrogen bonding, electrostatic interaction, and  $\pi$ - $\pi$  stacking, which, however, have not been fully confirmed. Nucleolar staining dyes such as SYTO RNASelect are favorable for fixed cells, while many CDs are capable of staining nucleoli in living cells.<sup>35,70</sup> Although the nucleolus-labeling CDs have been employed for applications of subcellular labeling, thermal sensing, and photothermal treatment, their use in diagnostic imaging of the nuclei, including the transformation processes, immune activation processes, and evaluation of chemo-drug treatment, has not been demonstrated, which are critical topics in nucleolus biology.



**2.4. Mitochondrion.** Mitochondria are the main source of intracellular ROS and reactive nitrogen species (RNS) and are involved in ROS/RNS-induced mycophagy and apoptosis.<sup>73</sup> The ROS/RNS may lead to increase in the oxidative stress and various metabolic changes that are associated with the development of neurological diseases, cardiovascular diseases, and cancer, among others.<sup>74</sup> Therefore, monitoring these endogenous and exogenous reactive species in mitochondria is important to understand the free-radical-related events. Fluorescent CDs with rich amino functional groups prepared from *o*-phenylenediamine and conjugated with triphenylphosphonium (TPP; mitochondria-targeting moiety) have been used to serve as a fluorescent probe for targeting mitochondria for sensing peroxynitrite (ONOO<sup>-</sup>) in living cells.<sup>75</sup> Peroxynitrite is an RNS that is highly harmful and can even damage biomolecules due to its oxidation and nitration ability. The amine-rich TPP-functionalized CDs (C-dots-TPP) as nanoprobe allow for the detection of peroxynitrite with a limit of detection (LOD) of 13.5 nM. The fluorescence of the CDs is quenched by peroxynitrite through photoinduced electron transfer. The biocompatibility and highly selective detection of peroxynitrite enable them for intracellular detection and long-time imaging. However, the C-dots-TPP nanoprobe cannot be used to sense the RNS in deep tissues due to their visible-light emission nature. CDs coupled with organelle-targeting moieties like TPP and morpholine have also been used to target mitochondria and lysosomes, respectively.<sup>76</sup> CDs can be functionalized with multiple probe molecules for increasing the detection efficiency through ratiometric signal acquisition. For example, TPP, amine, and coumarin-3-carboxylic acid (CCA)-functionalized CDs have been used as hybrid fluorescent nanosensors (CCA@TPP@CDs) for the detection of endogenous and exogenous hydroxyl radicals (<sup>•</sup>OH) in mitochondria in living cells.<sup>77</sup> In the hybrid, amine-functionalized CDs derived from 1,2,4-triaminobenzene exhibit yellow emission acting as the reference element, TPP functions as a mitochondrion-targeting molecule, and CCA functions as the <sup>•</sup>OH radical recognition moiety. The ratio of blue fluorescence from <sup>•</sup>OH radical-sensitive CCA components to yellow fluorescence from the <sup>•</sup>OH radical-independent CDs provides a reliable detection in mitochondria. The CCA@TPP@CD nanosensor is highly selective toward the <sup>•</sup>OH radical even in the presence of other ROS and biologically relevant cations.

A couple of studies have shown that some CDs can target mitochondria even without further modifications of the mitochondriotropic ligand such as TPP. The CDs prepared from chitosan, ethylenediamine, and mercaptosuccinic acid by a one-step hydrothermal method were employed for the imaging of mitochondria and mitochondria-targeted photodynamic cancer therapy.<sup>78</sup> Ultrasmall size (~2.1 nm), a positive charge of +28.1 mV, lipophilicity, and delocalized structure (benzene ring) of the CDs are the main reasons for their selective targeting of mitochondria. The cellular uptake of the CDs is energy-dependent and is involved in the caveolae-mediated endocytosis. These CDs, when coupled with a photosensitizer (Rose Bengal), can facilitate their internalization into the cells and serve as efficient materials for mitochondria-targeted PDT. Mitochondria have a very high membrane potential of up to -180 mV, leading to the tendency of accumulation of cationic species in the mitochondria rather than in other organelles. In addition, the negative membrane potentials of cancerous cells are higher than those of normal ones. Therefore, electrostatic-interaction-

dependent fluorescence properties of CDs can be utilized for the selective labeling of mitochondria in cancer cells in well-controlled staining concentration and time. Fluorescent CDs prepared from glycerol as a solvent and carbon source and (3-aminopropyl)trimethoxysilane (APTMS) as a passivation agent by a solvothermal treatment exhibit inherent mitochondrial targeting ability and the ability to differentiate cancerous cells from normal cells.<sup>79</sup> The differences in the membrane potentials and in the CDs' uptake efficiencies of normal cells and cancerous cells are contributors to the success. The electrostatic interaction of CDs with mitochondria affects their fluorescence intensity. Since the interaction of CDs with cancerous cells is stronger than with normal cells, a high fluorescence contrast was obtained in the former cells. Also, due to the high metabolic rate of cancerous cells, they consume more substances from the surrounding cells, which may also enhance their fluorescence due to their higher uptake of fluorescent CDs. After cell internalization, the CDs are highly stable and selective to target mitochondria rather than being captured by lysosomes.

ATP, the "energy currency", is produced mainly by mitochondria. The fluctuation in ATP production affects several physiological functions and is associated with many health issues such as aging, diabetes, Alzheimer's disease, hypercholesterolemia, and cardiovascular diseases.<sup>80</sup> Due to the similarity of this purine nucleotide with other nucleoside polyphosphates, selective monitoring of intracellular ATP is a challenge. Single-layered graphene CDs synthesized from the thermal condensation of perylene tetracarboxylic anhydride (PTCDA) and polyethylenimine (PEI), with strong yellow fluorescence, have been demonstrated to possess excellent targeting ability for mitochondria.<sup>81</sup> In addition, the graphene CDs are highly selective in differentiating ATP from other nucleoside polyphosphates due to the synergistic  $\pi$ - $\pi$  stacking and electrostatic interactions between the negatively charged purine nucleosides (exposed phosphate anions of ATP) and positively charged graphene CDs.<sup>81</sup> The graphene CDs were also used to monitor the mitochondrial ATP fluctuation in living cells induced by the Ca<sup>2+</sup> activation and sodium azide suppression.

CDs have also been used in the treatment of multidrug resistance (MDR) cancerous cells. MDR cancerous cells overexpress P-glycoprotein (P-gp), which captures and pumps the drugs from the cytoplasm to the extracellular space, reducing the accumulation of drugs in the cells and thereby lowering the therapeutic effect.<sup>82</sup> Zhang et al. developed a mitochondria-targeting nanomicelle-based drug delivery system to modulate P-gp and to efficiently release DOX inside cells.<sup>83</sup> Nanomicelle CDs-TPGS-TPP, prepared from fluorescent CDs and triphenylphosphine (TPP)-modified *D*- $\alpha$ -tocopheryl poly(ethylene glycol) succinate (TPGS) in an *n*-hexane/H<sub>2</sub>O mixed solution, were internalized into the cells through clathrin-mediated endocytosis and then targeted mitochondria specifically. TPP and TPGS inhibit the overexpression of P-gp and mitochondria targeting, respectively. The CDs-TPGS-TPP compared to free DOX causes a stronger depression in the mitochondrial membrane potential of MCF-7/ADR cells, reflecting the higher level of alterations of mitochondria DNA (mtDNA) caused by DOX released from the mitochondria-targeting nanocarriers. The targeting property of CDs-TPGS-TPP/DOX nanomicelles to mitochondria is promising for inducing apoptosis and damaging mtDNA in resistant MCF-7/ADR cells.

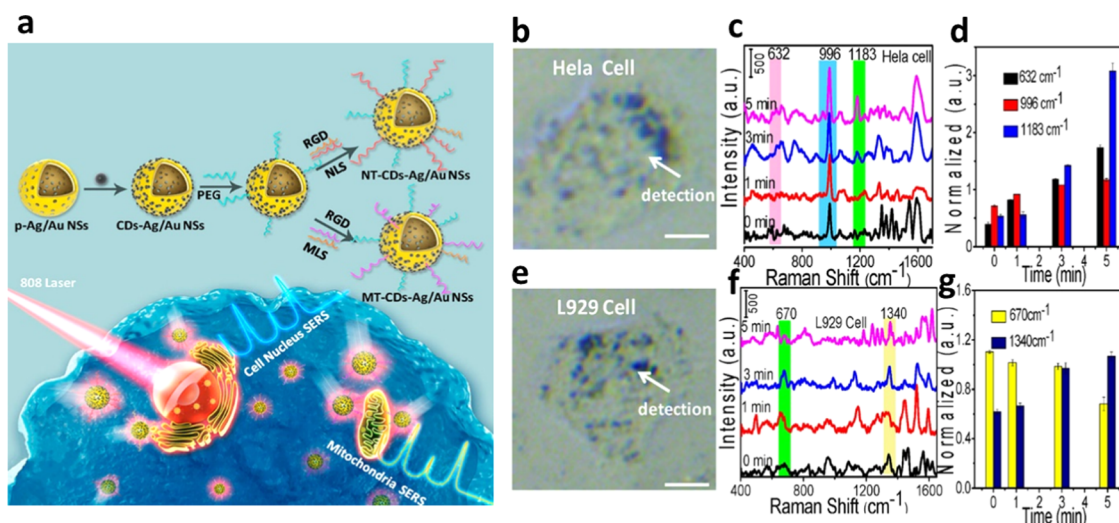


**Figure 6.** (a) Cartoon representation of the organelle-targeting theranostic plasmonic SERS nanoprobe (CDs–Ag/Au NSs). (b, e) Bright-field images and (c, f) their corresponding Raman spectra of HeLa cells and L929 cells after treatment with the SERS nanoprobe under NIR 808 nm laser exposure. (d, g) SERS intensity of different Raman bands for HeLa cells and L929 cells with different irradiation times under the PPT process. RGD is a cell-penetrating peptide (RGDRGDRGDRGDPGC), NLS is a nuclear-targeting peptide (GGVKKRKKKPGGC), and MLS is a mitochondria-targeting peptide (MLALLGWWWFSSRKKC). Reproduced with permission from ref 84. Copyright 2018 American Chemical Society.

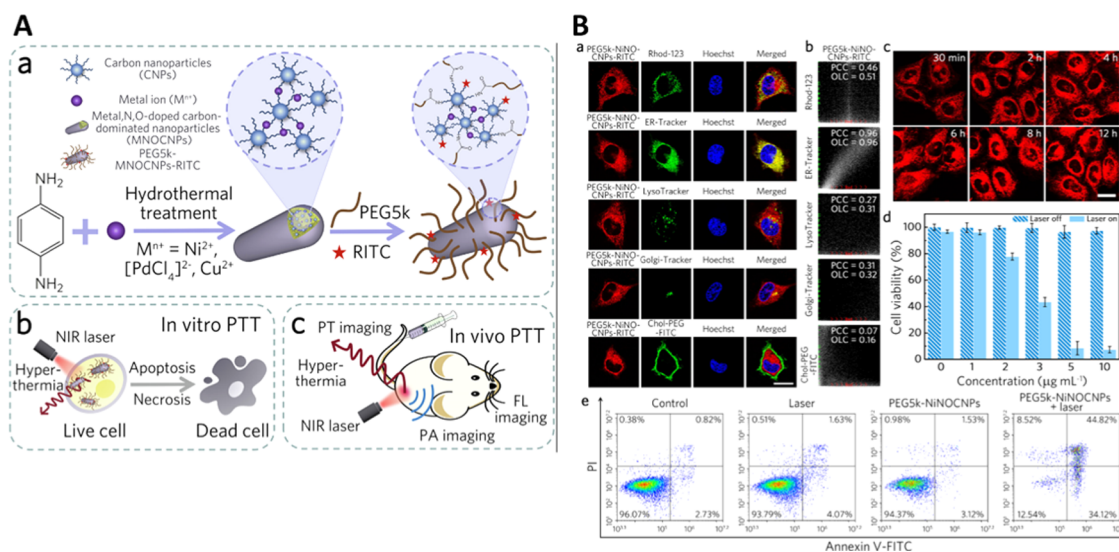


**Figure 7.** (A) Schematic representation displaying the (a) synthesis route of carbon nanoparticles doped with trace metal, N, and O (MNOCNPs) and functionalization with PEG, and their application in (b) *in vitro* PTT and (c) *in vivo* multimodal imaging of tumor ablation. (B) (a) Confocal fluorescence images of PEG- and rhodamine B isothiocyanate-modified MNOCNP (PEG5k-NiNOCNP-RITC)-treated HeLa cells costained with one of the different trackers and Hoechst. (b) Intensity correlation plots of PEG5k-NiNOCNPs-RITC and one of the trackers from (B, a). (c) Confocal fluorescence images of HeLa cells incubated with PEG5k-NiNOCNPs-RITC for different incubation times. (d) Cytotoxicity analysis of the modified CNPs toward HeLa cells with laser irradiation. (e) Apoptosis/necrosis assay results of HeLa cells subjected to different treatments. Reproduced with permission from ref 90. Copyright 2019 Acta Materialia Inc. Published by Elsevier Ltd.

A surface-enhanced Raman scattering (SERS) nanoprobe of porous Ag/Au nanoshells with surface decoration of CDs (CDs–Ag/Au NSs) was used for the nucleus- and mitochondria-targeted PTT of cancer cells (Figure 6).<sup>84</sup> The two peptides on the surfaces of the probe are responsible for specific targeting of mitochondria or nucleus. The nanoprobe absorbs NIR laser light for efficient killing of the cells during the PTT process as a result of boosting the light absorption capacity of the CD components. However, cancerous HeLa and normal (L929 and H8) cells show differences in molecular stress responses in PTT-induced cell death. The tryptophan,

phenylalanine, and tyrosine contents in HeLa cells are higher when compared to normal cells after the PTT process. The mitochondria-related cell apoptosis is due to cellular thermal stress-responsive proteins for HeLa cells and is related to DNA in the case of normal cells.

The difference in the membrane potential of mitochondria in cancerous cells to that of normal cells enables the labeling or drug delivery to mitochondria of cancer cells more easily. Various CDs have been developed as sensitive and selective probes for localization of mitochondria, mainly based on fluorescence quenching induced by the free radicals and

chemical species such as peroxyxynitrite. However, the fluorescence response of the CDs toward specific ROS or RNS inside the mitochondria must be investigated in detail for evaluating the state of mitochondria.

**2.5. Endoplasmic Reticulum.** Amine-functionalized CDs have been employed for the fluorescence imaging and pH sensing of organelles.<sup>33</sup> Shuang et al. demonstrated bioimaging of lysosomes and ER with pH-responsive CDs prepared from citric acid and urea by a hydrothermal method and then functionalized with laurylamine.<sup>33</sup> With an average size of 3 nm, the CDs without laurylamine and with laurylamine modification could monitor the pH fluctuations of lysosome and ER, respectively, mainly due to their differences in surface chemistry, cell internalization, and/or endocytosis pathways. The hydrophobic alkyl groups on the surface of laurylamine-modified CDs allow for their accelerated internalization and intracellular localization in ER through the lipid-raft-mediated endocytosis. The cellular endocytosis mechanisms of nanoparticles include clathrin-mediated endocytosis, caveolae-mediated endocytosis, and clathrin-/caveolae-independent endocytosis (e.g., macropinocytosis, phagocytosis, lipid-raft-dependent endocytosis).<sup>85</sup> Lipid rafts (10–200 nm) are the cellular membrane contained clusters of lipids in a more ordered state that exist within the generally disordered lipid milieu of the membrane.<sup>86</sup> Some nanoparticles are known to specifically bind to the lipid rafts of the cell membrane, and this binding may facilitate them to target the endoplasmic reticulum, following endocytosis to the endolysosomal machinery.<sup>87–89</sup> In the case of unmodified CDs, the amino groups interact with the cell membrane electrostatically and enter the cell through clathrin-mediated endocytosis and thus are localized in lysosomes.

In addition to organelle labeling, some CDs are efficient for ER-targeted therapy.<sup>90</sup> Multifunctional (trace metal-, N-, O-doped) carbon-dominated nanoparticles (MNOCNPs) conjugated with poly(ethylene glycol) (PEG) having high NIR absorption and biocompatibility were used for targeting of ER.<sup>90</sup> Figure 7A displays the synthesis of the multifunctional CDs and their application for PTT using an NIR laser. The carbon nanoparticles (CNPs) were formed during the hydrothermal treatment of phenylenediamine; simultaneously, the metal ions induced the cross-linking of CNPs to form the final photothermal MNOCNPs. The modification of MNOCNPs with PEG makes the nanoagents exhibit high physiological stability, enhanced cellular uptake, superior ER accumulation, and specific tumor-targeting capability. The PEG-MNOCNPs can also transport through the nuclear pores to interact with nucleoli upon NIR laser irradiation, leading to an effective PTT outcome even at a low drug dose (Figure 7B).

In summary, amine-functionalized CDs are found to be effective for the labeling of ER; however, they also label lysosomes. Moreover, aggregation and fluorescence responses of the CDs inside ER and lysosome could be different due to their environmental differences, including pH values. Thus, pH-dependent fluorescence properties of CDs must be studied in detail for monitoring of pH fluctuations in ER and lysosomes.

**2.6. Other Organelles.** Gold carbon dots (GCDs) with photoluminescent properties were employed for the fluorescence imaging of exosomes.<sup>91</sup> The GCDs conjugated with tumor-specific antibodies are specific for labeling the exosomes through immune reactions. The exosomes containing the

GCDs are then taken up by other cells and transported to lysosomes, which allows for the study of cancer metastasis. Li et al. showed that the chirality of CDs plays an important role in targeting the Golgi apparatus (Figure 8).<sup>92</sup> The fluorescent

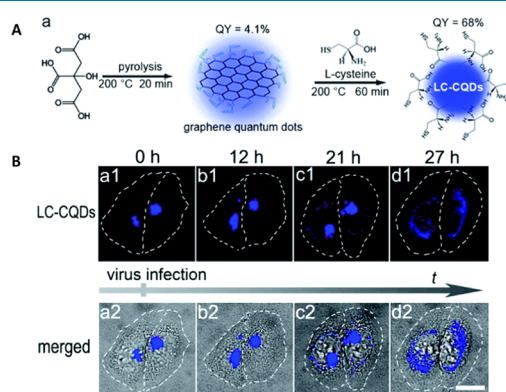


**Figure 8.** (A) Schematic representation of synthesis and functionalization of L-cysteine-modified CDs (LC-CQDs) from citric acid and L-cysteine and (B) LC-CQD-stained Golgi apparatus in HEp-2 cells during viral infection, showing morphological changes. Reproduced with permission from ref 92. Copyright 2017 Royal Society of Chemistry.

CDs were prepared from citric acid and L-cysteine (LC-CQDs) through two-step synthesis processes. Morphological changes of the Golgi apparatus are associated with intracellular injury like viral infections, and thus monitoring its change is important. On the other hand, CDs obtained from citric acid and D-cysteine by the same synthesis processes have limited targeting ability toward Golgi. The LC-CQDs likely bind to the sulfhydryl receptor site of the Golgi through the formation of disulfide bonds in the oxidizing environment of the Golgi lumen. However, the reason for the LC-CQDs' specificity toward the Golgi apparatus in the presence of a high concentration of intracellular thiols is unavailable. Nevertheless, this study demonstrated that the cellular uptake of LC-CQDs is energy-dependent and LC-CQDs can stain both *cis*- and *trans*-Golgi.<sup>92</sup> More importantly, the LC-CQDs can be used for long-term *in situ* imaging of Golgi without the generation of ROS. Although various CDs containing thiol functional groups with an L-stereo configuration were used for targeting Golgi,<sup>93–95</sup> a clear targeting mechanism is lacking.

### 3. FUTURE PERSPECTIVE AND CHALLENGES

A variety of CDs have been applied for labeling different subcellular structures; however, the targeting specificity of the CDs toward specific subcellular structures varies according to the precursors used in the syntheses and synthetic methods. Thus, the design and acquisition of CDs with subcellular labeling abilities and specificity are sometimes time-consuming and laborious. Although hydrophilicity is essential for CDs used for imaging applications,<sup>27</sup> hydrophobicity of CDs is found to be viable for labeling applications.<sup>48</sup> Taking advantage of the functional group-rich surface property, CDs can be potentially modified with various targeting ligands like antibodies for improving specificity toward the organelles. Due to their prominent photostability and strong fluorescence, they have gained popularity in monitoring drug delivery and/or monitoring therapeutic progresses. Although CDs have many advantages, the fluorescence QYs of CDs in many cases



are lower than those of traditional organic staining dyes. Under low-magnification imaging, the brightness of the CDs is sometimes insufficient, which disables effective subcellular imaging. Therefore, improving fluorescence QY of CDs will be beneficial for organelle labeling. PEI has been widely used for the surface modification of CDs for various bioapplications; however, lysosomes have been found to play a major role in mediating the toxicity of some PEI-functionalized CDs.<sup>96,97</sup> CDs synthesized from citric acid and functionalized with PEI have been found to decrease the viability of cells through oxidative stress and the interleukin (IL)-8 release mechanism.<sup>96</sup> Also, some CDs affect lysosome integrity and cause mitochondrial dysfunction and nucleotide-binding domain-like receptor protein 3 (NLRP3) inflammasome activation. Therefore, a detailed investigation of the cytotoxicity of CDs in various organelles is required.

CDs with strong interaction with DNA or RNA are found to be suitable for nuclear and nucleolar staining, respectively. Molecules with amino groups can easily penetrate into the cell through a diffusion process; however, they target many organelles. Functionalizing CDs with amines enables endocytosis *via* an active transportation mechanism, which results in enhanced targeted delivery or labeling of lysosomes. CDs must be properly functionalized with suitable functional molecules, for example, morpholine group (ML) and PEG have been employed to achieve high selectivity in targeting the lysosome and ER, respectively.<sup>26,90</sup> More studies to understand the internalization mechanism of CDs or drug-loaded CDs are needed. A correlation between the organelle-targeting property of CDs and functional groups or charges in the CDs is important to have ideal CDs for labeling of various organelles.

Some CDs, due to their unique surface functional properties, provide high selectivity toward cancerous cells over normal cells.<sup>45</sup> Organelle-specific targeting of CDs coupled with PTT holds great potential for monitoring the side effects during cancer therapy. It has been found that pH-dependent or NIR laser irradiation-induced release of the drugs from some CDs into cell organelles is efficient for inhibiting tumor growth; however, biosafety and biodistribution of the CDs must be investigated in more detail in the animal model.

Since various organelles have different pH values, a detailed study of the influence of pH on the  $\zeta$  potential, protonation/deprotonation, fluorescence, and aggregation properties of CDs is required to prepare ideal CDs for certain organelles. CDs are a great platform for multicolor labeling, either by their intrinsic fluorescence properties or by functionalizing with a fluorophore of different emission. The excitation-dependent fluorescence emission of CDs has been realized for multicolor fluorescence imaging in the visible-light range. However, the multicolor property of the CDs may cause a little problem when the cells are costained with other fluorophores that each only has a single fluorescent band. Overlapping of the fluorescence of the CDs and the fluorophore may result in indistinguishability between the two single sources. Thus, organic dyes with CDs must be selected carefully. For example, CDs usually having weak fluorescence in the long-wavelength region with organic dyes emitting in the NIR region are suitable to prevent the problem.

Development of CDs with single and narrow fluorescence properties is necessary to distinguish and track different groups of cells and to study intercellular interactions under coculture conditions. Preparation of CDs with pH- and temperature-sensitive fluorescence properties is important for real-time

monitoring of the pH and temperature fluctuations in organelles under different conditions like oxidative stress. To further improve imaging results, CDs possessing a sensitive fluorophore to pH changes and a stable fluorophore insensitive to pH changes are still welcome.

#### 4. CONCLUSIONS

This review concludes that fluorescent CDs are potential for labeling of organelles, with many advantages, including photostability, biocompatibility, easy preparation and functionalization, low cost, multicolor emission, small size, and rapid uptake. However, the potential of CDs for labeling of organelles has not been well realized. When compared to organic dyes, larger sizes of CDs are disadvantageous for high-resolution cell imaging. It is thus important to prepare ultrasmall CDs with a narrow size distribution and single and narrow fluorescence emission. We have found that CDs prepared through electrochemical approaches over hydrothermal ones provide a narrower size distribution.<sup>9</sup> CDs can be used for multicolor labeling and for developing ratiometric probes. With excellent photostability and ease of preparation, CDs provide opportunities for replacing organic dyes for specific organellar labeling. CDs for organelle labeling or targeted drug delivery into organelles without the use of any targeting agent or fluorophore can be achieved through careful selection of precursors that have a high affinity toward the organelles. However, well-defined design principles are still unavailable for preparing CDs with particular organelle-targeting properties; organelle labeling is usually achieved by applying a trial and error method. Labeling of organelles with CDs is always coupled with nonspecific cytoplasmic distribution, reducing the contrast of CD-labeled organelles. The highly stable fluorescent CDs for tracking the generations of cell division and cell proliferation analysis still remain a challenge. With high biocompatibility, the potential of CDs in live-cell imaging has been realized, but their use in animal models is rare. To make it more popular for animal studies, CDs with high QYs in the NIR and IR regions are needed. To prepare such CDs, doping of heterogeneous/metal atoms to CDs has shown to be a possible answer.

#### ■ AUTHOR INFORMATION

##### Corresponding Authors

**Chih-Ching Huang** – Department of Bioscience and Biotechnology and Center of Excellence for the Oceans, National Taiwan Ocean University, Keelung 20224, Taiwan; School of Pharmacy, College of Pharmacy, Kaohsiung Medical University, Kaohsiung 80708, Taiwan; [orcid.org/0000-0002-0363-1129](https://orcid.org/0000-0002-0363-1129); Email: [huanging@ntou.edu.tw](mailto:huanging@ntou.edu.tw)

**Huan-Tsung Chang** – Department of Chemistry, National Taiwan University, Taipei 10617, Taiwan; Department of Chemistry, Chung Yuan Christian University, Taoyuan City 32023, Taiwan; [orcid.org/0000-0002-5393-1410](https://orcid.org/0000-0002-5393-1410); Email: [changht@ntu.edu.tw](mailto:changht@ntu.edu.tw)

##### Authors

**Binesh Unnikrishnan** – Department of Bioscience and Biotechnology, National Taiwan Ocean University, Keelung 20224, Taiwan

**Ren-Siang Wu** – Department of Chemistry, National Taiwan University, Taipei 10617, Taiwan

**Shih-Chun Wei** – Department of Chemistry, National Taiwan University, Taipei 10617, Taiwan

Complete contact information is available at:  
<https://pubs.acs.org/10.1021/acsomega.9b04301>

## Notes

The authors declare no competing financial interest.

## ACKNOWLEDGMENTS

This study was supported by the Ministry of Science and Technology of Taiwan under the contracts 107-2113-M-002-015-MY3, 107-2113-M-019-004-MY3, and 108-2638-M-002-001-MY2.

## REFERENCES

- (1) Hu, F.; Liu, B. Organelle-specific bioprobes based on fluorogens with aggregation-induced emission (AIE) characteristics. *Org. Biomol. Chem.* **2016**, *14*, 9931–9944.
- (2) Gong, W.; Das, P.; Samanta, S.; Xiong, J.; Pan, W.; Gu, Z.; Zhang, J.; Qu, J.; Yang, Z. Redefining the photo-stability of common fluorophores with triplet state quenchers: mechanistic insights and recent updates. *Chem. Commun.* **2019**, *55*, 8695–8704.
- (3) Broadwater, D.; Bates, M.; Jayaram, M.; Young, M.; He, J.; Raithel, A. L.; Hamann, T. W.; Zhang, W.; Borhan, B.; Lunt, R. R.; Lunt, S. Y. Modulating cellular cytotoxicity and phototoxicity of fluorescent organic salts through counterion pairing. *Sci. Rep.* **2019**, *9*, No. 15288.
- (4) Cordes, T.; Maiser, A.; Steinhauer, C.; Schermelleh, L.; Tinnefeld, P. Mechanisms and advancement of antifading agents for fluorescence microscopy and single-molecule spectroscopy. *Phys. Chem. Chem. Phys.* **2011**, *13*, 6699–6709.
- (5) Kim, S.-W.; Roh, J.; Park, C.-S. Immunohistochemistry for pathologists: protocols, pitfalls, and tips. *J. Pathol. Transl. Med.* **2016**, *50*, 411–418.
- (6) Hsu, P.-C.; Chang, H.-T. Synthesis of high-quality carbon nanodots from hydrophilic compounds: role of functional groups. *Chem. Commun.* **2012**, *48*, 3984–3986.
- (7) Molaei, M. J. Carbon quantum dots and their biomedical and therapeutic applications: a review. *RSC Adv.* **2019**, *9*, 6460–6481.
- (8) Hsu, P.-C.; Shih, Z.-Y.; Lee, C.-H.; Chang, H.-T. Synthesis and analytical applications of photoluminescent carbon nanodots. *Green Chem.* **2012**, *14*, 917–920.
- (9) Wang, C.-I.; Wu, W.-C.; Periasamy, A. P.; Chang, H.-T. Electrochemical synthesis of photoluminescent carbon nanodots from glycine for highly sensitive detection of hemoglobin. *Green Chem.* **2014**, *16*, 2509–2514.
- (10) Dekaliuk, M.; Pyshev, K.; Demchenko, A. Visualization and detection of live and apoptotic cells with fluorescent carbon nanoparticles. *J. Nanobiotechnol.* **2015**, *13*, No. 86.
- (11) Roy, P.; Chen, P.-C.; Periasamy, A. P.; Chen, Y.-N.; Chang, H.-T. Photoluminescent carbon nanodots: synthesis, physicochemical properties and analytical applications. *Mater. Today* **2015**, *18*, 447–458.
- (12) Xu, D.; Lin, Q.; Chang, H.-T. Recent advances and sensing applications of carbon dots. *Small Methods* **2020**, No. 1900387.
- (13) Barbosa, C. D. d. E. S.; Corrêa, J. R.; Medeiros, G. A.; Barreto, G.; Magalhães, K. G.; de Oliveira, A. L.; Spencer, J.; Rodrigues, M. O.; Neto, B. A. D. Carbon dots (c-dots) from cow manure with impressive subcellular selectivity tuned by simple chemical modification. *Chem. – Eur. J.* **2015**, *21*, 5055–5060.
- (14) Hsu, P.-C.; Chen, P.-C.; Ou, C.-M.; Chang, H.-Y.; Chang, H.-T. Extremely high inhibition activity of photoluminescent carbon nanodots toward cancer cells. *J. Mater. Chem. B* **2013**, *1*, 1774–1781.
- (15) Liu, M. L.; Chen, B. B.; Li, C. M.; Huang, C. Z. Carbon dots: synthesis, formation mechanism, fluorescence origin and sensing applications. *Green Chem.* **2019**, *21*, 449–471.
- (16) Kasouni, A.; Chatzimitakos, T.; Stalikas, C. Bioimaging applications of carbon nanodots: a review. *C J. Carbon Res.* **2019**, *5*, No. 19.
- (17) Pirsahab, M.; Mohammadi, S.; Salimi, A.; Payandeh, M. Functionalized fluorescent carbon nanostructures for targeted imaging of cancer cells: a review. *Microchim. Acta* **2019**, *186*, No. 231.
- (18) Du, J.; Xu, N.; Fan, J.; Sun, W.; Peng, X. Carbon dots for in vivo bioimaging and theranostics. *Small* **2019**, *15*, No. 1805087.
- (19) Jiang, K.; Sun, S.; Zhang, L.; Lu, Y.; Wu, A.; Cai, C.; Lin, H. Red, green, and blue luminescence by carbon dots: full-color emission tuning and multicolor cellular imaging. *Angew. Chem., Int. Ed.* **2015**, *54*, 5360–5363.
- (20) Yao, Z.; Lai, Z.; Chen, C.; Xiao, S.; Yang, P. Full-color emissive carbon-dots targeting cell walls of onion for in situ imaging of heavy metal pollution. *Analyst* **2019**, *144*, 3685–3690.
- (21) Singh, V.; Rawat, K. S.; Mishra, S.; Baghel, T.; Fatima, S.; John, A. A.; Kalleti, N.; Singh, D.; Nazir, A.; Rath, S. K.; Goel, A. Biocompatible fluorescent carbon quantum dots prepared from beetroot extract for in vivo live imaging in *C. elegans* and BALB/c mice. *J. Mater. Chem. B* **2018**, *6*, 3366–3371.
- (22) Zhi, B.; Cui, Y.; Wang, S.; Frank, B. P.; Williams, D. N.; Brown, R. P.; Melby, E. S.; Hamers, R. J.; Rosenzweig, Z.; Fairbrother, D. H.; Orr, G.; Haynes, C. L. Malic acid carbon dots: from super-resolution live-cell imaging to highly efficient separation. *ACS Nano* **2018**, *12*, 5741–5752.
- (23) Nandi, S.; Malishev, R.; Bhunia, S. K.; Kolusheva, S.; Jopp, J.; Jelinek, R. Lipid-bilayer dynamics probed by a carbon dot-phospholipid conjugate. *Biophys. J.* **2016**, *110*, 2016–2025.
- (24) Song, Y.; Li, H.; Lu, F.; Wang, H.; Zhang, M.; Yang, J.; Huang, J.; Huang, H.; Liu, Y.; Kang, Z. Fluorescent carbon dots with highly negative charges as a sensitive probe for real-time monitoring of bacterial viability. *J. Mater. Chem. B* **2017**, *5*, 6008–6015.
- (25) Du, F.; Li, J.; Hua, Y.; Zhang, M.; Zhou, Z.; Yuan, J.; Wang, J.; Peng, W.; Zhang, L.; Xia, S.; Wang, D.; Yang, S.; Xu, W.; Gong, A.; Shao, Q. Multicolor nitrogen-doped carbon dots for live cell imaging. *J. Biomed. Nanotechnol.* **2015**, *11*, 780–788.
- (26) Wu, L.; Li, X.; Ling, Y.; Huang, C.; Jia, N. Morpholine derivative-functionalized carbon dots-based fluorescent probe for highly selective lysosomal imaging in living cells. *ACS Appl. Mater. Interfaces* **2017**, *9*, 28222–28232.
- (27) Zhang, Q. Q.; Yang, T.; Li, R. S.; Zou, H. Y.; Li, Y. F.; Guo, J.; Liu, X. D.; Huang, C. Z. A functional preservation strategy for the production of highly photoluminescent emerald carbon dots for lysosome targeting and lysosomal pH imaging. *Nanoscale* **2018**, *10*, 14705–14711.
- (28) Kang, Y.-F.; Fang, Y.-W.; Li, Y.-H.; Li, W.; Yin, X.-B. Nucleus-staining with biomolecule-mimicking nitrogen-doped carbon dots prepared by a fast neutralization heat strategy. *Chem. Commun.* **2015**, *51*, 16956–16959.
- (29) Jung, Y. K.; Shin, E.; Kim, B.-S. Cell nucleus-targeting zwitterionic carbon dots. *Sci. Rep.* **2015**, *5*, No. 18807.
- (30) Lai, I. P.-J.; Harroun, S. G.; Chen, S.-Y.; Unnikrishnan, B.; Li, Y.-J.; Huang, C.-C. Solid-state synthesis of self-functional carbon quantum dots for detection of bacteria and tumor cells. *Sens. Actuators, B* **2016**, *228*, 465–470.
- (31) Sri, S.; Kumar, R.; Panda, A. K.; Solanki, P. R. Highly biocompatible, fluorescence, and zwitterionic carbon dots as a novel approach for bioimaging applications in cancerous cells. *ACS Appl. Mater. Interfaces* **2018**, *10*, 37835–37845.
- (32) Yuan, F.; Li, Y.; Li, X.; Zhu, J.; Fan, L.; Zhou, S.; Zhang, Y.; Zhou, J. Nitrogen-rich D- $\pi$ -A structural carbon quantum dots with a bright two-photon fluorescence for deep-tissue imaging. *ACS Appl. Bio Mater.* **2018**, *1*, 853–858.
- (33) E, S.; Mao, Q.-X.; Yuan, X.-L.; Kong, X.-L.; Chen, X.-W.; Wang, J.-H. Targeted imaging of the lysosome and endoplasmic reticulum and their pH monitoring with surface regulated carbon dots. *Nanoscale* **2018**, *10*, 12788–12796.
- (34) Wang, H.; Wang, X. *In vitro* nucleus nanoprobe with ultra-small polyethylenimine functionalized graphene quantum dots. *RSC Adv.* **2015**, *5*, 75380–75385.

- (35) Zhu, Z.; Li, Q.; Li, P.; Xun, X.; Zheng, L.; Ning, D.; Su, M. Surface charge controlled nucleoli selective staining with nanoscale carbon dots. *PLoS One* **2019**, *14*, No. e0216230.
- (36) Kumawat, M. K.; Thakur, M.; Gurung, R. B.; Srivastava, R. Graphene quantum dots for cell proliferation, nucleus imaging, and photoluminescent sensing applications. *Sci. Rep.* **2017**, *7*, No. 15858.
- (37) Hua, X.-W.; Bao, Y.-W.; Wu, F.-G. Fluorescent carbon quantum dots with intrinsic nucleolus-targeting capability for nucleolus imaging and enhanced cytosolic and nuclear drug delivery. *ACS Appl. Mater. Interfaces* **2018**, *10*, 10664–10677.
- (38) Xue, Z.; Zhao, H.; Liu, J.; Han, J.; Han, S. Imaging lysosomal pH alteration in stressed cells with a sensitive ratiometric fluorescence sensor. *ACS Sens.* **2017**, *2*, 436–442.
- (39) Kallunki, T.; Olsen, O. D.; Jäättelä, M. Cancer-associated lysosomal changes: friends or foes? *Oncogene* **2013**, *32*, 1995–2004.
- (40) Xiang, H.-J.; Guo, M.; An, L.; Yang, S.-P.; Zhang, Q.-L.; Liu, J.-G. A multifunctional nanoplatform for lysosome targeted delivery of nitric oxide and photothermal therapy under 808 nm near-infrared light. *J. Mater. Chem. B* **2016**, *4*, 4667–4674.
- (41) Singh, H.; Sreedharan, S.; Tiwari, K.; Green, N. H.; Smythe, C.; Pramanik, S. K.; Thomas, J. A.; Das, A. Two photon excitable graphene quantum dots for structured illumination microscopy and imaging applications: lysosome specificity and tissue-dependent imaging. *Chem. Commun.* **2019**, *55*, 521–524.
- (42) Chen, S.; Jia, Y.; Zou, G.-Y.; Yu, Y.-L.; Wang, J.-H. A ratiometric fluorescent nanoprobe based on naphthalimide derivative-functionalized carbon dots for imaging lysosomal formaldehyde in HeLa cells. *Nanoscale* **2019**, *11*, 6377–6383.
- (43) Liu, H.; Sun, Y.; Li, Z.; Yang, J.; Aryee, A. A.; Qu, L.; Du, D.; Lin, Y. Lysosome-targeted carbon dots for ratiometric imaging of formaldehyde in living cells. *Nanoscale* **2019**, *11*, 8458–8463.
- (44) Unzeta, M.; Solé, M.; Boada, M.; Hernández, M. Semi-carbazide-sensitive amine oxidase (SSAO) and its possible contribution to vascular damage in Alzheimer's disease. *J. Neural Transm.* **2007**, *114*, 857–862.
- (45) Duong, A.; Steinmaus, C.; McHale, C. M.; Vaughan, C. P.; Zhang, L. Reproductive and developmental toxicity of formaldehyde: a systematic review. *Mutat. Res., Rev. Mutat. Res.* **2011**, *728*, 118–138.
- (46) Pontel, L. B.; Rosado, I. V.; Burgos-Barragan, G.; Garaycochea, J. I.; Yu, R.; Arends, M. J.; Chandrasekaran, G.; Broecker, V.; Wei, W.; Liu, L.; Swenberg, J. A.; Crossan, G. P.; Patel, K. J. Endogenous formaldehyde is a hematopoietic stem cell genotoxin and metabolic carcinogen. *Mol. Cell* **2015**, *60*, 177–188.
- (47) He, Y.; Li, Z.; Jia, Q.; Shi, B.; Zhang, H.; Wei, L.; Yu, M. Ratiometric fluorescent detection of acidic pH in lysosome with carbon nanodots. *Chin. Chem. Lett.* **2017**, *28*, 1969–1974.
- (48) Mao, Q.-X.; E, S.; Xia, J.-M.; Song, R.-S.; Shu, Y.; Chen, X.-W.; Wang, J.-H. Hydrophobic carbon nanodots with rapid cell penetrability and tunable photoluminescence behavior for in vitro and in vivo imaging. *Langmuir* **2016**, *32*, 12221–12229.
- (49) Wu, F.; Chen, J.; Li, Z.; Su, H.; Leung, K. C.-F.; Wang, H.; Zhu, X. Red/near-infrared emissive metalloporphyrin-based nanodots for magnetic resonance imaging-guided photodynamic therapy in vivo. *Part. Part. Syst. Charact.* **2018**, *35*, No. 1800208.
- (50) Zhang, D.-Y.; Zheng, Y.; Zhang, H.; He, L.; Tan, C.-P.; Sun, J.-H.; Zhang, W.; Peng, X.; Zhan, Q.; Ji, L.-N.; Mao, Z.-W. Ruthenium complex-modified carbon nanodots for lysosome-targeted one- and two-photon imaging and photodynamic therapy. *Nanoscale* **2017**, *9*, 18966–18976.
- (51) Hill, S. A.; Sheikh, S.; Zhang, Q.; Sueiro Ballesteros, L.; Herman, A.; Davis, S. A.; Morgan, D. J.; Berry, M.; Benito-Alifonso, D.; Galan, M. C. Selective photothermal killing of cancer cells using LED-activated nucleus targeting fluorescent carbon dots. *Nanoscale Adv.* **2019**, *1*, 2840–2846.
- (52) Yang, L.; Jiang, W.; Qiu, L.; Jiang, X.; Zuo, D.; Wang, D.; Yang, L. One pot synthesis of highly luminescent polyethylene glycol anchored carbon dots functionalized with a nuclear localization signal peptide for cell nucleus imaging. *Nanoscale* **2015**, *7*, 6104–6113.
- (53) Ci, J.; Tian, Y.; Kuga, S.; Niu, Z.; Wu, M.; Huang, Y. One-pot green synthesis of nitrogen-doped carbon quantum dots for cell nucleus labeling and copper(II) detection. *Chem. – Asian J.* **2017**, *12*, 2916–2921.
- (54) Yuan, Y.; Guo, B.; Hao, L.; Liu, N.; Lin, Y.; Guo, W.; Li, X.; Gu, B. Doxorubicin-loaded environmentally friendly carbon dots as a novel drug delivery system for nucleus targeted cancer therapy. *Colloids Surf., B* **2017**, *159*, 349–359.
- (55) Shi, L.; Li, Y.; Li, X.; Wen, X.; Zhang, G.; Yang, J.; Dong, C.; Shuang, S. Facile and eco-friendly synthesis of green fluorescent carbon nanodots for applications in bioimaging, patterning and staining. *Nanoscale* **2015**, *7*, 7394–7401.
- (56) Liu, H.; Bai, Y.; Zhou, Y.; Feng, C.; Liu, L.; Fang, L.; Liang, J.; Xiao, S. Blue and cyan fluorescent carbon dots: one-pot synthesis, selective cell imaging and their antiviral activity. *RSC Adv.* **2017**, *7*, 28016–28023.
- (57) Dai, Q.; Zhao, H.; Cao, H.; Yang, J.; Zhao, W.; Wang, T.; Liu, L.; Fan, Z.; Wang, G. Photo-triggered conversion of hydrophilic fluorescent biomimetic nanostructures for cell imaging. *Chem. Commun.* **2019**, *55*, 596–599.
- (58) Zhang, J.; Zhao, X.; Xian, M.; Dong, C.; Shuang, S. Folic acid-conjugated green luminescent carbon dots as a nanoprobe for identifying folate receptor-positive cancer cells. *Talanta* **2018**, *183*, 39–47.
- (59) Duan, Q.; Che, M.; Hu, S.; Zhao, H.; Li, Y.; Ma, X.; Zhang, W.; Zhang, Y.; Sang, S. Rapid cancer diagnosis by highly fluorescent carbon nanodots-based imaging. *Anal. Bioanal. Chem.* **2019**, *411*, 967–972.
- (60) Yang, J.; Gao, G.; Zhang, X.; Ma, Y.-H.; Jia, H.-R.; Jiang, Y.-W.; Wang, Z.; Wu, F.-G. Ultrasmall and photostable nanotheranostic agents based on carbon quantum dots passivated with polyamine-containing organosilane molecules. *Nanoscale* **2017**, *9*, 15441–15452.
- (61) Farley, K. I.; Surovtseva, Y.; Merkel, J.; Baserga, S. J. Determinants of mammalian nucleolar architecture. *Chromosoma* **2015**, *124*, 323–331.
- (62) Penzo, M.; Montanaro, L.; Treré, D.; Derenzini, M. The ribosome biogenesis-cancer connection. *Cells* **2019**, *8*, No. 55.
- (63) Gupta, A. S.; Sengupta, K. Lamin B2 modulates nucleolar morphology, dynamics, and function. *Mol. Cell Biol.* **2017**, *37*, No. e00274-17.
- (64) Stimpson, K. M.; Sullivan, L. L.; Kuo, M. E.; Sullivan, B. A. Nucleolar organization, ribosomal DNA array stability, and acrocentric chromosome integrity are linked to telomere function. *PLoS One* **2014**, *9*, No. e92432.
- (65) Lara-Martínez, R.; De Lourdes Segura-Valdez, M.; De La Mora-De La Mora, I.; López-Velázquez, G.; Jiménez-García, L. F. Morphological studies of nucleologenesis in *Giardia lamblia*. *Anat. Rec.* **2016**, *299*, 549–556.
- (66) Cao, C.; Wei, P.; Li, R.; Zhong, Y.; Li, X.; Xue, F.; Shi, Y.; Yi, T. Ribosomal RNA-selective light-up fluorescent probe for rapidly imaging the nucleolus in live cells. *ACS Sens.* **2019**, *4*, 1409–1416.
- (67) Feng, R.; Li, L.; Li, B.; Li, J.; Peng, D.; Yu, Y.; Mu, Q.; Zhao, N.; Yu, X.; Wang, Z. Turn-on fluorescent probes that can light up endogenous RNA in nucleoli and cytoplasm of living cells under a two-photon microscope. *RSC Adv.* **2017**, *7*, 16730–16736.
- (68) Khan, S.; Verma, N. C.; Chethana; Nandi, C. K. Carbon Dots for single-molecule imaging of the nucleolus. *ACS Appl. Nano Mater.* **2018**, *1*, 483–487.
- (69) Hua, X.-W.; Bao, Y.-W.; Zeng, J.; Wu, F.-G. Nucleolus-targeted red emissive carbon dots with polarity-sensitive and excitation-independent fluorescence emission: High-resolution cell imaging and in vivo tracking. *ACS Appl. Mater. Interfaces* **2019**, *11*, 32647–32658.
- (70) Han, G.; Zhao, J.; Zhang, R.; Tian, X.; Liu, Z.; Wang, A.; Liu, R.; Liu, B.; Han, M.-Y.; Gao, X.; Zhang, Z. Membrane-penetrating carbon quantum dots for imaging nucleic acid structures in live organisms. *Angew. Chem., Int. Ed.* **2019**, *58*, 7087–7091.
- (71) Li, H.; Zhang, M.; Song, Y.; Wang, H.; Liu, C.; Fu, Y.; Huang, H.; Liu, Y.; Kang, Z. Multifunctional carbon dot for lifetime thermal



sensing, nucleolus imaging and anti-algal activity. *J. Mater. Chem. B* **2018**, *6*, 5708–5717.

(72) Sun, S.; Zhang, L.; Jiang, K.; Wu, A.; Lin, H. Toward high-efficient red emissive carbon dots: facile preparation, unique properties, and applications as multifunctional theranostic agents. *Chem. Mater.* **2016**, *28*, 8659–8668.

(73) Bolisetty, S.; Jaimes, E. A. Mitochondria and reactive oxygen species: physiology and pathophysiology. *Int. J. Mol. Sci.* **2013**, *14*, 6306–6344.

(74) Liguori, I.; Russo, G.; Curcio, F.; Bulli, G.; Aran, L.; Della-Morte, D.; Gargiulo, G.; Testa, G.; Cacciatore, F.; Bonaduce, D.; Abete, P. Oxidative stress, aging, and diseases. *Clin. Interventions Aging* **2018**, *13*, 757–772.

(75) Wu, X.; Sun, S.; Wang, Y.; Zhu, J.; Jiang, K.; Leng, Y.; Shu, Q.; Lin, H. A fluorescent carbon-dots-based mitochondria-targetable nanoprobe for peroxynitrite sensing in living cells. *Biosens. Bioelectron.* **2017**, *90*, 501–507.

(76) Wu, X.; Ma, L.; Sun, S.; Jiang, K.; Zhang, L.; Wang, Y.; Zeng, H.; Lin, H. A versatile platform for the highly efficient preparation of graphene quantum dots: photoluminescence emission and hydrophilicity–hydrophobicity regulation and organelle imaging. *Nanoscale* **2018**, *10*, 1532–1539.

(77) Zhou, D.; Huang, H.; Wang, Y.; Wang, Y.; Hu, Z.; Li, X. A yellow-emissive carbon nanodot-based ratiometric fluorescent nanosensor for visualization of exogenous and endogenous hydroxyl radicals in the mitochondria of live cells. *J. Mater. Chem. B* **2019**, *7*, 3737–3744.

(78) Hua, X.-W.; Bao, Y.-W.; Chen, Z.; Wu, F.-G. Carbon quantum dots with intrinsic mitochondrial targeting ability for mitochondria-based theranostics. *Nanoscale* **2017**, *9*, 10948–10960.

(79) Gao, G.; Jiang, Y.-W.; Yang, J.; Wu, F.-G. Mitochondria-targetable carbon quantum dots for differentiating cancerous cells from normal cells. *Nanoscale* **2017**, *9*, 18368–18378.

(80) Gorman, G. S.; Chinnery, P. F.; DiMauro, S.; Hirano, M.; Koga, Y.; McFarland, R.; Suomalainen, A.; Thorburn, D. R.; Zeviani, M.; Turnbull, D. M. Mitochondrial diseases. *Nat. Rev. Dis. Primers* **2016**, *2*, No. 16080.

(81) Liu, J. H.; Li, R. S.; Yuan, B.; Wang, J.; Li, Y. F.; Huang, C. Z. Mitochondria-targeting single-layered graphene quantum dots with dual recognition sites for ATP imaging in living cells. *Nanoscale* **2018**, *10*, 17402–17408.

(82) Nanayakkara, A. K.; Follit, C. A.; Chen, G.; Williams, N. S.; Vogel, P. D.; Wise, J. G. Targeted inhibitors of P-glycoprotein increase chemotherapeutic-induced mortality of multidrug resistant tumor cells. *Sci. Rep.* **2018**, *8*, No. 967.

(83) Zhang, Y.; Zhang, C.; Chen, J.; Liu, L.; Hu, M.; Li, J.; Bi, H. Trackable mitochondria-targeting nanomicellar loaded with doxorubicin for overcoming drug resistance. *ACS Appl. Mater. Interfaces* **2017**, *9*, 25152–25163.

(84) Qi, G.; Zhang, Y.; Xu, S.; Li, C.; Wang, D.; Li, H.; Jin, Y. Nucleus and mitochondria targeting theranostic plasmonic surface-enhanced Raman spectroscopy nanoprobes as a means for revealing molecular stress response differences in hyperthermia cell death between cancerous and normal cells. *Anal. Chem.* **2018**, *90*, 13356–13364.

(85) Foroozandeh, P.; Aziz, A. A. Insight into cellular uptake and intracellular trafficking of nanoparticles. *Nanoscale Res. Lett.* **2018**, *13*, No. 339.

(86) Sezgin, E.; Levental, I.; Mayor, S.; Eggeling, C. The mystery of membrane organization: composition, regulation and roles of lipid rafts. *Nat. Rev. Mol. Cell Biol.* **2017**, *18*, 361–374.

(87) Chakraborty, A.; Jana, N. R. Clathrin to lipid raft-endocytosis via controlled surface chemistry and efficient perinuclear targeting of nanoparticle. *J. Phys. Chem. Lett.* **2015**, *6*, 3688–3697.

(88) El-Sayed, A.; Harashima, H. Endocytosis of gene delivery vectors: from clathrin-dependent to lipid raft-mediated endocytosis. *Mol. Ther.* **2013**, *21*, 1118–1130.

(89) Li, Y.; Gao, L.; Tan, X.; Li, F.; Zhao, M.; Peng, S. Lipid raft-mediated endocytosis and physiology-based cell membrane traffic

models of doxorubicin liposomes. *Biochim. Biophys. Acta, Biomembr.* **2016**, *1858*, 1801–1811.

(90) Bao, Y.-W.; Hua, X.-W.; Li, Y.-H.; Jia, H.-R.; Wu, F.-G. Endoplasmic reticulum-targeted phototherapy using one-step synthesized trace metal-doped carbon-dominated nanoparticles: laser-triggered nucleolar delivery and increased tumor accumulation. *Acta Biomater.* **2019**, *88*, 462–476.

(91) Jiang, X.; Zong, S.; Chen, C.; Zhang, Y.; Wang, Z.; Cui, Y. Gold–carbon dots for the intracellular imaging of cancer-derived exosomes. *Nanotechnology* **2018**, *29*, No. 175701.

(92) Li, R. S.; Gao, P. F.; Zhang, H. Z.; Zheng, L. L.; Li, C. M.; Wang, J.; Li, Y. F.; Liu, F.; Li, N.; Huang, C. Z. Chiral nanoprobes for targeting and long-term imaging of the Golgi apparatus. *Chem. Sci.* **2017**, *8*, 6829–6835.

(93) Wang, L.; Wu, B.; Li, W.; Li, Z.; Zhan, J.; Geng, B.; Wang, S.; Pan, D.; Wu, M. Industrial production of ultra-stable sulfonated graphene quantum dots for Golgi apparatus imaging. *J. Mater. Chem. B* **2017**, *5*, 5355–5361.

(94) Yuan, M.; Guo, Y.; Wei, J.; Li, J.; Long, T.; Liu, Z. Optically active blue-emitting carbon dots to specifically target the Golgi apparatus. *RSC Adv.* **2017**, *7*, 49931–49936.

(95) Li, C. H.; Li, R. S.; Li, C. M.; Huang, C. Z.; Zhen, S. J. Precise ricin A-chain delivery by Golgi-targeting carbon dots. *Chem. Commun.* **2019**, *55*, 6437–6440.

(96) Ronzani, C.; Van Belle, C.; Didier, P.; Spiegelhalter, C.; Pierrat, P.; Lebeau, L.; Pons, F. Lysosome mediates toxicological effects of polyethyleneimine-based cationic carbon dots. *J. Nanopart. Res.* **2018**, *21*, No. 4.

(97) Havrdova, M.; Hola, K.; Skopalik, J.; Tomankova, K.; Petr, M.; Cepe, K.; Polakova, K.; Tucek, J.; Bourlinos, A. B.; Zboril, R. Toxicity of carbon dots – Effect of surface functionalization on the cell viability, reactive oxygen species generation and cell cycle. *Carbon* **2016**, *99*, 238–248.